Research article

Hypoxia triggers cardiomyocyte apoptosis via regulating the m^{6}A methylation-mediated LncMIAT/miR-708-5p/p53 axis

Chuqiao Shen [a], Xiaoqi Chen [b], Yixuan Lin [b], Yan Yang [a,*]

[a] *Department of Pharmacology, School of Basic Medical Science, Anhui Medical University, Hefei, Anhui, 230012, PR China*
[b] *Graduate School, Anhui University of Chinese Medicine, Hefei, Anhui, 230012, PR China*

ARTICLE INFO

ABSTRACT

Long-time hypoxia induced cardiomyocyte apoptosis is an important mechanism of myocardial ischemia (MI) injury. Interestingly, long noncoding RNA myocardial infarction-associated transcript (LncMIAT) has been involved in the regulation of MI injury; however, the underlying mechanism by which LncMIAT affects the progression of hypoxia-induced cardiomyocyte apoptosis remains unclear. In the present study, hypoxia was found to promote cardiomyocyte apoptosis through an increased expression of LncMIAT *in vitro*. Biological investigations and dual-luciferase gene reporter assay further revealed that LncMIAT was able to bind with miR-708-5p to upregulate the p53-mediated cell death of the cardiomyocytes. Silencing of LncMIAT or over-expression of miR-708-5p led to a significant reduction in p53-mediated cardiomyocyte apoptosis. The methylated RNA immunoprecipition (MeRIP)-qPCR results showed that hypoxia exerted its effects on LncMIAT through AKLBH5-N^6-methyladenosine (m^{6}A) methylation and therefore hypoxia was shown to trigger HL-1 cardiomyocyte apoptosis via the m^{6}A methylation-mediated LncMIAT/miR-708-5p/p53 axis. Silencing of AKLBH5 significantly alleviated the m^{6}A methylation-mediated LncMIAT upregulation and p53-mediated cardiomyocyte apoptosis, while promoted miR-708-5p expression. Taken together, the present study highlighted that LncMIAT could act as a key biological target during hypoxia-induced cardiomyocyte apoptosis. In addition, it was shown that hypoxia could promote cardiomyocyte apoptosis through regulation of the m^{6}A methylation-mediated LncMIAT/miR-708-5p/p53 signaling axis.

1. Introduction

Ischemic heart disease is associated with high mortality rates worldwide [1]. Patients who have ischemic heart disease without receiving effective treatment for the condition end up developing heart failure, with gradual cardiovascular death [2]. Generally, myocardial hypoxia is the major cause underlying ischemic heart disease. The mechanism(s) underlying myocardial ischemia (MI) and myocardial hypoxia were shown to comprise the energy metabolism dysfunction [3], apoptosis [4] and necrosis [5] of cardiomyocytes. Notably, myocardial apoptosis was shown to fulfil an important role in acute MI both in the clinical [6] and in animal research [7]. However, although myocardial apoptosis was shown to be associated with MI progression, the mechanism governing how MI influences myocardial apoptosis remains unclear.

---

* Corresponding author. Department of Pharmacology, School of Basic Medical Science, 81 Meishan Road, Anhui Medical University, Anhui, 230012, PR China.
E-mail address: yangyan@ahmu.edu.cn (Y. Yang).

Myocardial apoptosis is generally mediated through caspase-dependent regulation [8]. Briefly, myocardial intracellular apoptosis is activated through changes in the levels of the death signaling-induced mitochondrial proteins, Bax and Bcl-2, followed by the triggering of apoptosis through the conversion of procaspase into caspase-3 [9,10]. P53 was reported to be a mediator of hypoxia-induced myocardial apoptosis [11,12], which provides a further mechanism for regulating Bax and caspase-3-mediated cardiomyocyte apoptosis [13–15]. However, it is presently unknown how the hypoxia stimulus regulates p53-induced cardiomyocyte apoptosis and further studies are required to delineate details of the precise underlying mechanisms that exist between hypoxia and p53.

Interestingly, long noncoding (lnc)RNA myocardial infarction-associated transcript (LncMIAT) has been newly identified as an ncRNA biomarker in the blood samples of patients with MI [16,17]. In an animal model, LncMIAT was shown to be positively correlated with myocardial injury indicators, including creatine kinase-MB (CK-MB) and cardiac troponin T (cTnT) [18]. LncMIAT was also shown to impair myocardial contractility in an MI mouse model [19], which was associated with heart failure and cardiac hypotrophy in a LncMIAT-knockout mouse model [20]. To determine whether or not LncMIAT is correlated with MI, the present study analyzed the bioinformatics data of LncMIAT in MI blood samples from Gene Expression Omnibus (GEO) datasets. Moreover, the LncMIAT level in cardiomyocytes was measured under hypoxic conditions.

LncMIAT was shown to be associated with the apoptosis pathway in cardiomyocytes. A previous study demonstrated that downregulating expression of LncMIAT ameliorated ischemic injury and minimized myocardial cell apoptosis through upregulation of p53 [21,22]. However, how LncMIAT regulates p53-induced apoptosis in cardiomyocytes under hypoxic conditions remains unclear. Although LncMIAT is unable to directly regulate apoptosis, certain studies established that the endogenous RNA axis exerts a regulatory role on apoptotic mechanisms [23,24]. Recently, it was discovered that the miRNA miR-708-5p could protect cardiomyocytes from hypoxia-induced damage [25] and apoptosis under hypoxic conditions [26]. To understand the association between LncMIAT and miR-708-5p, and miR-708-5p and p53 mRNA, the present study provided and validated the predicted RNA-binding sites, according to their RNA sequences. To further assess the effects of LncMIAT under hypoxic conditions, it was noted that the N^6-methyladenosine (m^6A) methylation modification gained attention with respect to LncMIAT modulation, especially in studies on myocardium disease [27,28]. Moreover, a decrease in m^6A methylation was shown to be mediated via the upregulation of ALKB homolog H5 (ALKBH5) demethylase in post-ischemic cardiovascular endothelial cells [29]. These studies suggested that ALKBH5 demethylase might affect the m^6A methylation of LncMIAT. Therefore, the present study investigated the m^6A methylation level and enzyme function of ALKBH5 demethylase with respect to alterations of LncMIAT in cardiomyocytes under hypoxic conditions. Hypoxia was established in an HL-1 cardiac muscle cell line to establish an MI *in vitro* model. It was hypothesized that a hypoxia stimulus may lead to cardiomyocyte apoptosis through regulating alterations in the m^6A methylation-induced LncMIAT/miR-708-5p/p53 signaling axis. Taken together, the results of the present study may provide a theoretical and experimental basis for MI-induced myocardial apoptosis.

2. Materials and methods

2.1. LncMIAT expression data acquisition

The present study analyzed data from five MI samples and five control samples deposited on the Gene Expression Omnibus (GEO) database (https://www.ncbi.nlm.nih.gov/geo/) under accession no. GSE48060 (https://www.ncbi.nlm.nih.gov/geo/query/acc.cgi?acc=GSE48060). The expression value was analyzed using the interactive GEO web tool GEO2R (https://www.ncbi.nlm.nih.gov/geo/geo2r/). Heatmap and box-plot analyses were performed using R 3.6.1 (Revolution Analytics) with the packages 'pheatmap' and 'limma'. Adjusted (adj.)P < 0.05 and |log fold change (logFC)| >1.0 were chosen as the criteria to identify differentially expressed genes (DEGs).

2.2. Cell culture, transfection and establishment of the in vitro hypoxic cell model

The HL-1 cell lines were provided by the BeNa Culture Collection (cat no. BNCC288890; BNCC), and cells were incubated in DMEM (cat no. SH30022.01B; Hyclone) supplemented with 10 % FBS (cat no. 10270-106; Gibco; Thermo Fisher Scientific, Inc.). 293T cells were provided by the Shanghai Institute of Biochemistry and Cell Biology (cat no. SCSP-502). The cells were incubated at 37 °C in a constant atmosphere of 5 % CO_2.

For the plasmid transfection process, cells were transfected with short interfering (si)RNA targeting MIAT (Si-MIAT) or ALKBH5

Table 1
Si-LncMIAT, Si-ALKBH5 and miR-708-5p mimic and inhibitor sequences.

Identifier	Sense	Anti-sense
Si-LncMIAT	5′-GCCCUACUAACUGGUUUCUTT-3′	5′-AGAAACCAGUUAGUAGGGCTT-3′
Si-NC	5′-UUCUCCGAACGUGUCACGUTT-3′	5′-ACGUGACACGUUCGGAGAATT-3′
Si-ALKBH5	5′-GCUGCAAGUUCCAGUUCAATT-3′	5′-UUGAACUGGAACUUGCAGCTT-3′
miR-708-5p mimic	5′-AAGGAGCUUACAAUCUAGCUGGG-3′	5′-CAGCUAGAUUGUAAGCUCCUUUU-3′
miR-708-5p inhibitor	5′-CCCAGCUAGAUUGUAAGCUCCUU-3′	NONE
mimic-NC	5′-UUCUCCGAACGUGUCACGUTT-3′	5′-ACGUGACACGUUCGGAGAATT-3′
inhibitor-NC	5′-CAGUACUUUUGUGUAGUACAA-3′	NONE

(Si-ALKBH5), negative control (NC) siRNA (Si-NC), miR-708-5p mimic, miR-708-5p inhibitor, miR-708-5p mimic-NC and miR-708-5p inhibitor-NC. The siRNA sequences are listed in Table 1. The cells were transfected at 70–80 % confluence using an Invitrogen™ Lipofectamine™ 2000 Kit (cat no. 11668-027; Thermo Fisher Scientific, Inc.), according to the manufacturer's instructions. The cells were incubated at 37 °C for 48 h before determining the transfection efficiency.

For hypoxia cell treatment, the cells were incubated under a humidified atmosphere of 95 % N_2 and 5 % CO_2 to simulate MI in an *in vitro* model. The cells were incubated at 37 °C under the aforementioned hypoxic conditions for 24 h.

2.3. Establishment of the in vivo MI mouse model and subsequent treatments

A total of 15 8-week-old C57BL/6 male mice were obtained from Hangzhou Ziyuan Experimental Animal Technology Co., Ltd. All mice were given free access to water and food, and were housed in a room at a controlled temperature and humidity with a 12-h light/dark cycle. All experimental protocols were approved by the Animal Experimentation Ethics Committee of the Anhui University of Chinese Medicine (approval no. AHUCM-mouse-2022009) and conducted following the EU Directive 2010/63/EU guideline [30]. MI mouse model was induced by ligating the left anterior descending (LAD) according to previous study [31]. Before the operation, the mice in the SHAM and MI groups were intragastrically administered 0.9 % sodium chloride solution, whereas mice in the MI + IOX1 group were intragastrically administered the ALKBH5 inhibitor IOX1 (cat no. HY-12304; MedChemExpress), at a dose of 20 mg/kg/day for 12 days [32,33]. After 24 h ligation, all the mice were euthanized via intraperitoneal injection of 1 % pentobarbital sodium (150 mg/kg) followed by cervical dislocation to minimize discomfort and pain.

2.4. Histological analysis

Ventricle tissue slices (thickness, 2 mm) were fixed with 4 % neutral paraformaldehyde at room temperature for 36 h and then embedded with paraffin. The heart slices were then cut into 5-μm paraffin sections and stained with hematoxylin at room temperature for 3 min and eosin at room temperature for 30 s. Histopathological changes in the cardiomyocytes were observed under an optical microscope.

2.5. TUNEL assay for the detection of myocardial apoptosis

Myocardial apoptosis of the heart slices was evaluated through TUNEL staining with 3,3-diaminobenzidine (DAB). According to the manufacturer's instructions provided with the kit (cat. no. C1098; Beyotime Institute of Biotechnology), the heart slices were prepared with TUNEL detection solution (5 μl terminal deoxynucleotidyl transferase enzyme and 45 μl Biotin-deoxyuridine triphosphate) and incubated at 37 °C for 60 min. Subsequently, the slices were incubated at room temperature with the streptavidin-HRP working solution (50 μl) for 30 min, followed by incubation with DAB and hematoxylin for nuclear staining at room temperature for 10 min. Apoptosis of the cardiomyocytes was detected using a Nikon Eclipse 50i microscope (Nikon Corporation).

2.6. Reverse transcription-quantitative (RT-q)PCR analysis

Total RNA was isolated from cardiomyocytes (1×10^7 cells) using the TRIzol™ reagent (cat. no. 15596018; Thermo Fisher Scientific, Inc.) and reverse transcribed into cDNA using an Applied Biosystems™ High-Capacity cDNA Reverse Transcription Kit (Thermo Fisher Scientific, Inc.). The extraction of cDNA for qPCR was performed using the SYBR-Green qPCR Master Mix (cat. no. G3322-05; Wuhan Servicebio Technology Co., Ltd.). The qPCR thermocycling conditions were as follows: Initial denaturation at 95 °C for 30 s; followed by 40 cycles of denaturation at 95 °C for 15 s, and 40 cycles of annealing at 60 °C for 30 s. All PCRs were performed in triplicate using the Bio-Rad Chromo 4™ System qPCR System (cat. no. PTC0200G; Bio-Rad Laboratories, Inc.). The RNA level was measured using the $2^{-\Delta\Delta Cq}$ method, with β-actin and U6 serving as the endogenous controls. The primers for qPCR were designed based on the NCBI Primer-BLAST System and are listed in Table 2.

Table 2
Primer sequences for reverse transcription-quantitative PCR.

Identifier	Forward primer	Reverse primer
β-actin	5′-AGTGTGACGTTGACATCCGT-3′	5′-TGCTAGGAGCCAGAGCAGTA-3′
U6	5′-CTCGCTTCGGCAGCACA-3′	5′-AACGCTTCACGAATTTGCGT-3′
P53	5′-GAACCGCCGACCTATCCTTA-3′	5′-CACGAACCTCAAAGCTGTCC-3′
Bax	5′-AGGATGATTGCTGACGTGGA-3′	5′-CCCAGTTGAAGTTGCCATCA-3′
Bcl-2	5′-AGGCAAATGGTCGAATCAGC-3′	5′-GGCAATTCCTGGTTCGGTTT-3′
Caspase-3	5′-CACGTGGGAAAGTGAACCAG-3′	5′-CTGGCCCTTTCGTTTCTAGC-3′
LncMIAT	5′-AAAGGTCACGACTAGCCTGC-3′	5′-AGCTGACCCTTTCTCACACG-3′
Mir-708-5p	GCGCGAAGGAGCTTACAATCTA-3′	5′-AGTGCAGGGTCCGAGGTATT-3′
Mir-708-5p reverse transcription primer	5′-GTCGTATCCAGTGCAGGGTCCGAGGTATTCGCACTGGATACGACCCCAGC-3′	
ALKBH5	5′-GTGACTGTGCTCAGTGGGTA-3′	5′-GGCGATCTGAAGCATAGCTG-3′

2.7. Western blotting

Proteins were fractionated using RIPA cell lysate buffer (containing 1 mM PMSF), before being separated by SDS/PAGE on 10 % gels. Subsequently, the proteins were transferred onto PVDF membranes. The membranes were incubated with the primary anti-Bcl-2 (1:2000; cat. no. ab182858; Abcam), anti-Bax (1:1000; cat. no. ab32503, Abcam), anti-caspase-3 (cat. no. ab184787; 1:2000; Abcam), anti-cleaved caspase-3 (cat. no. 341034; 1:1000; ZENBIO), anti-hypoxia-inducible factor (HIF)-1α (cat. no. AF1009; 1:500; Affinity Biosciences), anti-p53 (cat. no. AF0879; 1:1000; Affinity Biosciences), anti-ALKBH5 (cat. no. DF2585; 1:1000; Affinity Biosciences) antibodies and β-actin (cat. no. TA-09; 1:1000; Zs-BIO) at 4 °C overnight. Next, the blotted membranes were incubated for 2 h with the HRP-conjugated secondary antibodies (cat. no. ZB-2305; 1:8000; and cat. no. ZB-2301; 1:5000; Zs-BIO) at ambient temperature. ECL reagent (MilliporeSigma) was used to visualize the protein bands using β-actin as a loading control.
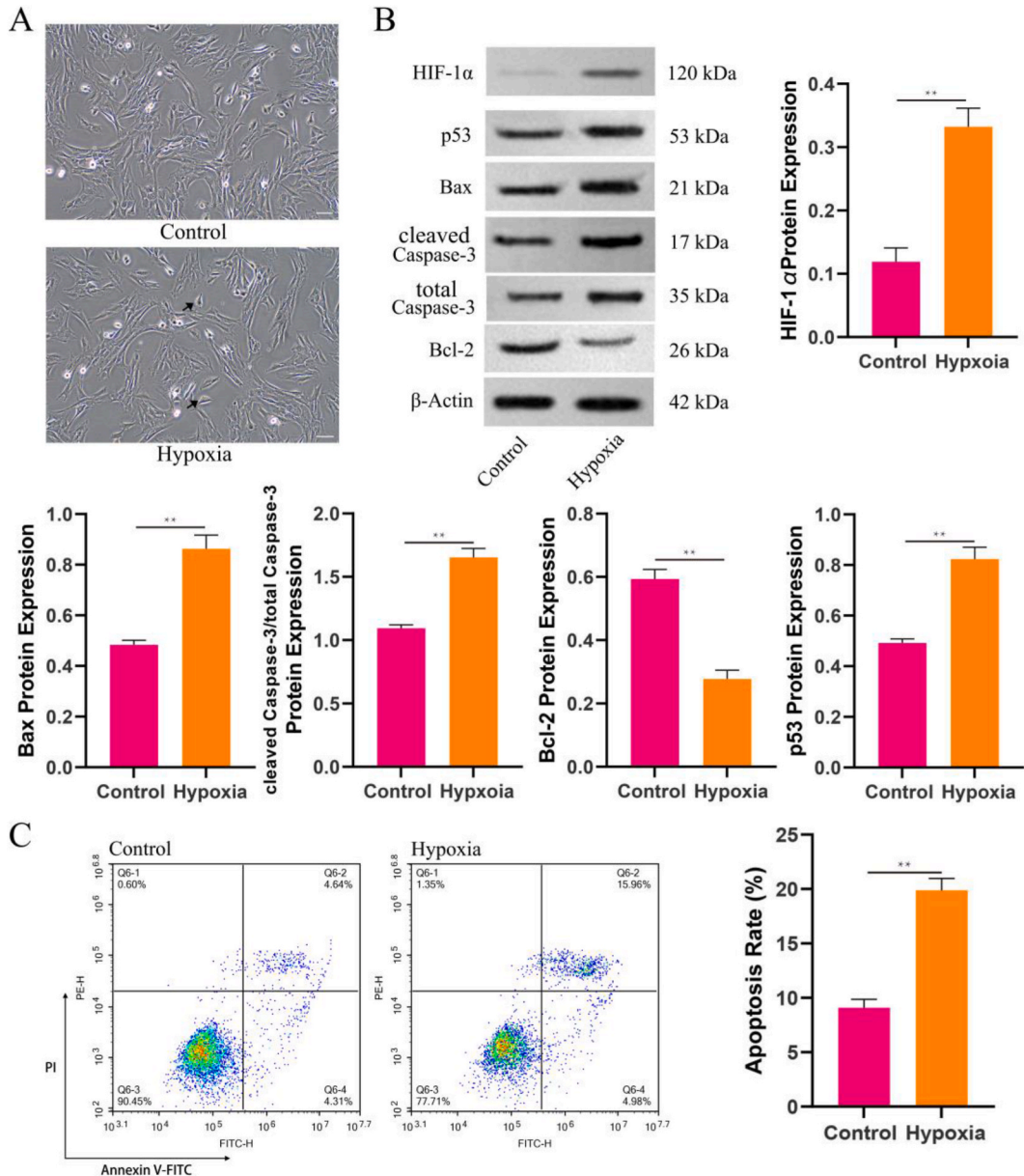

Fig. 1. Hypoxia promotes HL-1 cardiomyocyte apoptosis. (A) Morphological microscopy images of normoxic control and hypoxic HL-1 cells (scale bar, 50 μm; cell shrinkage is shown by the black arrows). (B) Relative protein expression levels of HIF-1α, P53, Bax, cleaved Caspase-3 and Bcl-2 are shown. (C) The apoptotic rate of HL-1 cells under hypoxic condition through flow cytometry. Data are shown as the mean ± standard deviation (n = 3). **P < 0.01 vs. control group.

2.8. m⁶A RNA methylation quantification

Total RNA was isolated from the myocardium of mice using the TRIzol reagent. The total m^6A level of the mRNA was detected using an EpiQuik m^6A RNA Methylation Quantification Kit (colorimetric kit; cat. no. P-9005-48; EpiGentek), following the manufacturer's instructions.

2.9. Flow cytometric analysis

HL-1 cells (1×10^6) were digested with 0.25 % trypsin and centrifuged for cells collection. Apoptosis was measured using an Annexin V-FITC-PI apoptosis detection kit (cat. no. CA1020; Solarbio). Fluorescence signals and apoptosis rates were examined using flow cytometry. Data analysis was performed using the NovoExpress Software v1.6.1 (Agilent Technologies, Inc.).

2.10. Dual-luciferase assay

The wild-type (WT) (p53-WT and LncMIAT-WT-containing binding sites for miR-708-5p) and mutant (MUT) plasmids (p53-MUT and LncMIAT-MUT) were consolidated into a psiCHECK-2 vector (Tongyong Biotechnology Co., Ltd.). 293T cells (5×10^3) were cultured on 96-well plates and then co-transfected with WT/MUT luciferase plasmids or miR-708-5p mimic/mimic NC for 48 h by using transfection reagent Lipofectamine 2000™ (cat. no. 11668-027; Invitrogen; Thermo Fisher Scientific, Inc.). After 48 h transfection at room temperature, luciferase activity was measured using a Dual Luciferase Reporter Gene Assay Kit (cat. no. RG027; Beyotime Institute of Biotechnology) and an EnSpire multimode microplate reader (PerkinElmer, Inc.), according to the manufacturer's protocol. Firefly luciferase activity was normalized to *Renilla* luciferase activity.
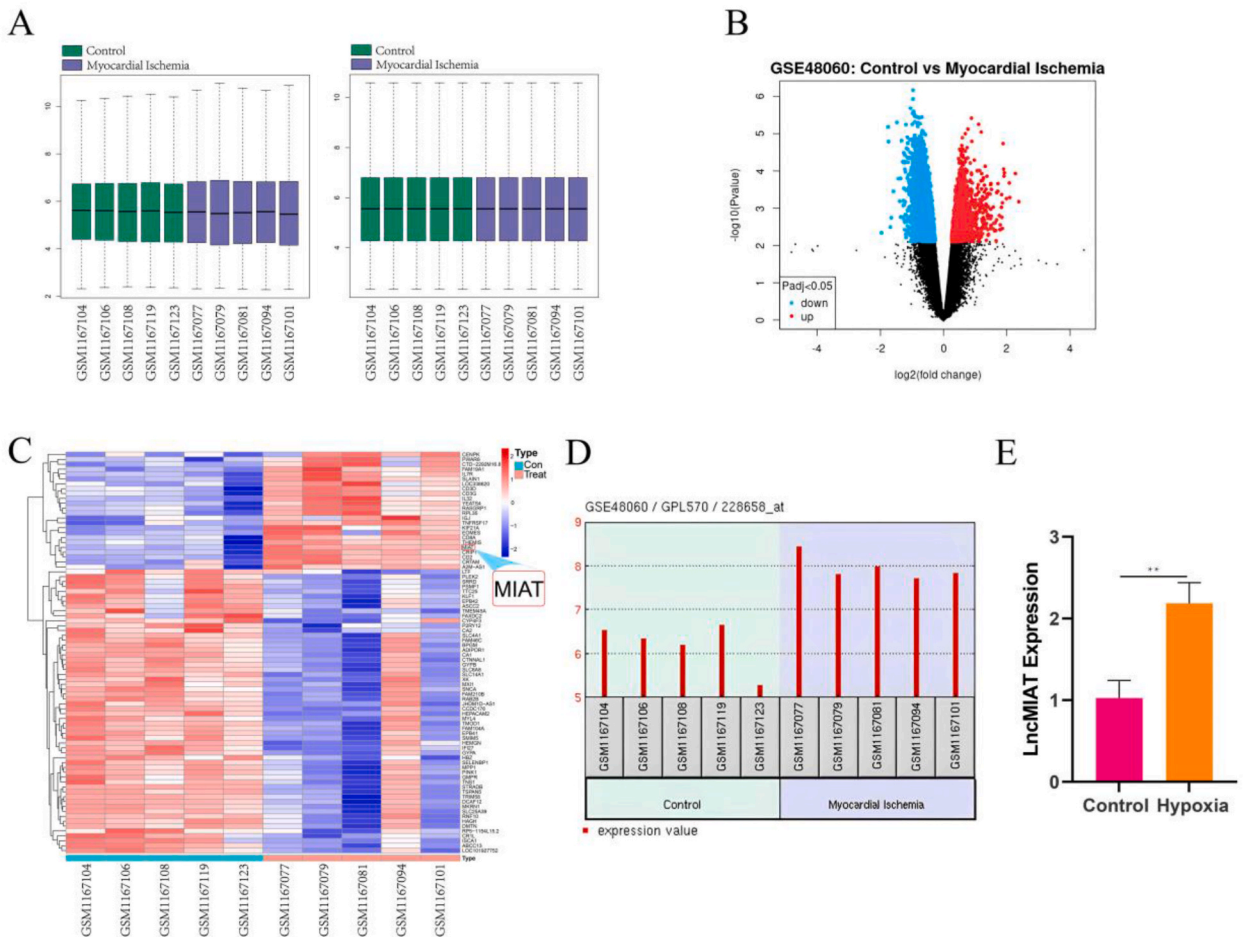

Fig. 2. Hypoxia stimulus significantly increases the expression of LncMIAT in HL-1 cells. (A) Raw and normalized box plots of DEGs in GSE48060 samples. (B) Volcano plots of DEGs in GSE48060 samples. (C) Heatmaps of DEGs in the samples of patients with MI analyzed using R 3.6.1 with the software package 'pheatmap'. (D) Representative LncMIAT expression value of patients with MI. (E) Relative LncMIAT expression in hypoxic HL-1 cells. Data are presented as the mean ± standard deviation (n ≥ 3). **P < 0.01 vs. control group.

2.11. Methylated RNA immunoprecipitation sequencing (MeRIP)-qPCR

A Magna MeRIP™ m^{6}A Kit (cat. no. 17–10499; MilliporeSigma) was used to perform RNA methylation immunoprecipitation. Total RNA was isolated from cardiomyocytes (1×10^7) by using 1 mL TRIzol™ reagent. The RNA (10 μg) was fragmented into small nucleotides and then immunoprecipitated using magnetic beads (2 μl) with m^{6}A antibodies (2 μl) (Synaptic Systems). After the collection of the m^{6}A eluent, RT-qPCR was used to detect the LncMIAT level, as aforementioned.

2.12. Statistical analysis

All results are shown as the mean ± standard deviation. Student's t-test was performed for comparisons between two groups, whereas one-and two-way ANOVA analysis was performed followed by the Tukey's post hoc test to evaluate the significant differences between each group with multiple comparisons. Statistical data were analyzed using SPSS 22.0 software (IBM Corp.). P < 0.05 indicates that the difference is statistically significant, and P < 0.01 was considered to indicate a statistically significant difference.

3. Results

3.1. Hypoxia promotes cardiomyocyte apoptosis in an HL-1 cell model

The present study aimed to explore the effects of hypoxia on HL-1 cardiomyocyte apoptosis *in vitro*. The HL-1 cardiomyocytes were treated under hypoxic conditions for 24 h. Compared with the control group, the HL-1 cells exhibited shrinkage under the hypoxic regime (Fig. 1A). The HIF-1α level was found to be significantly enhanced in the hypoxia group (P < 0.01; Fig. 1B), indicating that the hypoxic HL-1 cardiomyocyte model had been successfully established. The p53 (P < 0.01; Fig. 1B), Bax (P < 0.01; Fig. 1B) and cleaved Caspase-3 (P < 0.01; Fig. 1B) protein expression levels in the hypoxia group were also significantly elevated compared with those in
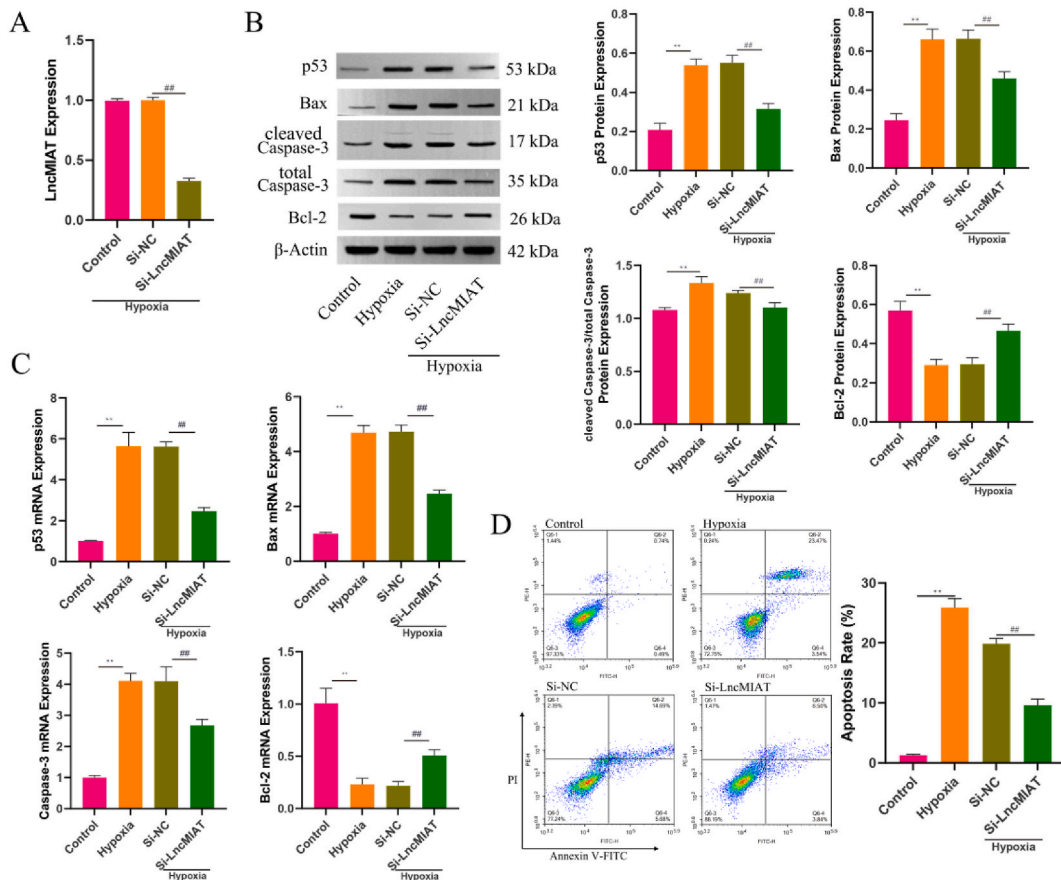

Fig. 3. Silencing of long noncoding RNA myocardial infarction-associated transcript decreases hypoxia-induced cardiomyocyte apoptosis in HL-1 cells. (A) Relative LncMIAT expression in Si-LncMIAT and Si-NC treatments of hypoxic HL-1 cells. (B) Relative protein expression levels of P53, Bax, cleaved Caspase-3 and Bcl-2. (C) Relative mRNA expression levels of P53, Bax, Caspase-3 and Bcl-2. (D) Apoptotic rate of HL-1 cells according to flow cytometric analysis. The data are shown as the mean ± standard deviation (n ≥ 3). **P < 0.01 vs. control group. ##P < 0.01 vs. Si-NC group.

the control group. By contrast, the Bcl-2 (P < 0.01; Fig. 1B) protein expression level in the hypoxia group were significantly decreased compared with those in the control group. Fig. 1C demonstrates that hypoxia was associated with an increased rate of apoptosis of the cardiomyocytes, according to the Annexin-V/PI flow cytometric analysis.

3.2. The hypoxia stimulus significantly increases LncMIAT expression in MI patients and cardiomyocytes

The data of patients with MI were retrieved from the GEO dataset, accession no. GSE48060. The box-plot analysis, showing the statistical normalization of all data, is featured in Fig. 2A. Fig. 2B shows a volcano plot, featuring 82 DEGs (including 24 upregulated and 58 downregulated DEGs), according to the criteria adj. P < 0.05 and |logFC| >1.0. The adj. P and |logFC| values for LncMIAT were determined to be 0.0137 and 1.416, respectively. Hierarchical clustering analysis showed that the expression levels of the 24 upregulated genes, including LncMIAT, were significantly increased in MI samples compared with those in the control group (Fig. 2C). According to the GEO2R analysis, the LncMIAT expression values of the patients with MI were found to be upregulated compared with those in the control group (Fig. 2D). RT-qPCR results showed the hypoxia stimulus led to a significant upregulation of LncMIAT compared with control (P < 0.01; Fig. 2E).

3.3. LncMIAT regulates cardiomyocyte apoptosis under hypoxic conditions

In the subsequent set of experiments, cardiomyocytes were transfected with Si-LncMIAT to investigate whether LncMIAT could affect cardiomyocyte apoptosis following the hypoxic stimulus. The effects of both Si-LncMIAT and Si-NC transfection were investigated in the hypoxic HL-1 cell model. The expression of LncMIAT was significantly decreased in the Si-LncMIAT group compared with that in the Si-NC group (P < 0.01; Fig. 3A). The mRNA and protein expression levels of p53 (P < 0.01; Fig. 3B and C) and Bax (P < 0.01; Fig. 3B and C) were decreased in the Si-LncMIAT group compared with those in the Si-NC group. The protein expression level of cleaved Caspase-3 (P < 0.01; Fig. 3B) and mRNA expression level of Caspase-3 (P < 0.01; Fig. 3C) were decreased in the Si-LncMIAT group compared with those in the Si-NC group. By contrast, the mRNA and protein expression levels of Bcl-2 (P < 0.01; Fig. 3B and C)
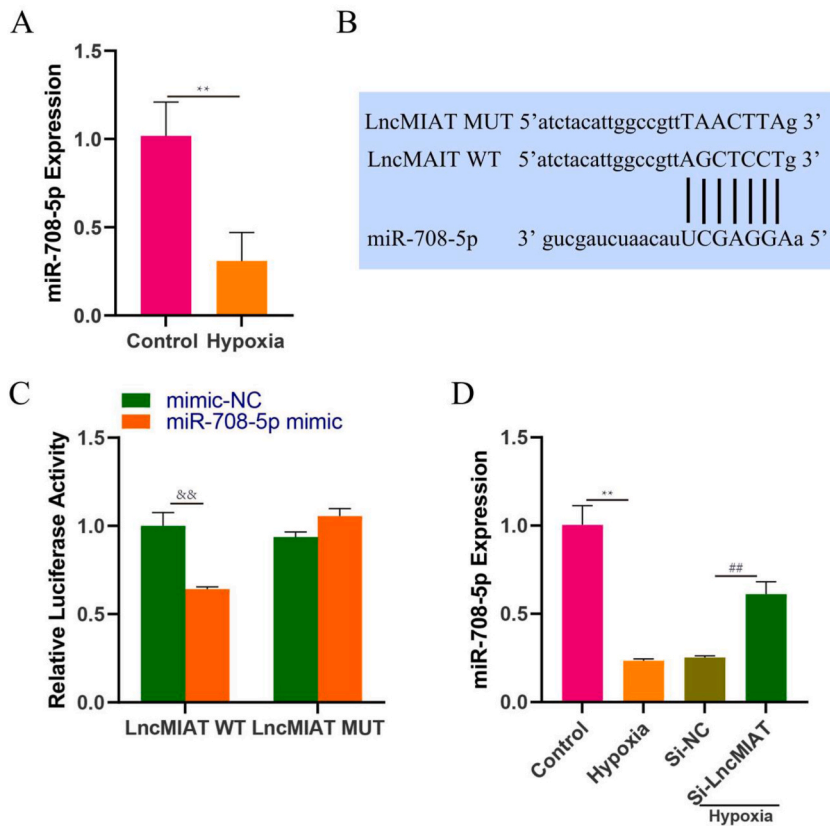

Fig. 4. LncMIAT regulates miR-708-5p in hypoxic HL-1 cells. (A) MiR-708-5p mRNA expression was measured using RT-qPCR analysis. (B) Predicted binding site of miR-708-5p with MIAT and mutant sequence of MIAT. (C) Binding of miR-708-5p to LncMIAT was detected using the dual luciferase reporter assay. (D) Treatment with Si-LncMIAT led to an increase in the mRNA expression of miR-708-5p, as detected using RT-qPCR analysis. Data are shown as the mean ± standard deviation (n ≥ 3). **P < 0.01 vs. control group. &&P < 0.01 vs. mimic-NC group. ##P < 0.01 vs. Si-NC group.

were increased compared with the Si-NC group. According to the Annexin-V/PI flow cytometric assay, the Si-LncMIAT group showed a decrease in the apoptotic ratio compared with the Si-NC group (P < 0.01; Fig. 3D).

3.4. LncMIAT endogenously binds with miR-708-5p and regulates miR-708-5p expression in hypoxic cardiomyocytes

Compared with the control group, the establishment of hypoxia led to a downregulation of miR-708-5p (P < 0.01; Fig. 4A) in the hypoxia group. Fig. 4B depicts the predicted binding site of miR-708-5p to LncMIAT, and the LncMIAT mutation sequence (LncMIAT MUT). To confirm the association of miR-708-5p with LncMIAT, a dual-luciferase gene report assay was employed, which demonstrated that the luciferase activity was significantly decreased following transfection with LncMIAT-WT and a miR-708-5p mimic, but not with LncMIAT-MUT and a miR-708-5p mimic (P < 0.01; Fig. 4C). Subsequently, the miR-708-5p expression level was further validated in the Si-LncMIAT and Si-NC groups. As shown in Fig. 4D, miR-708-5p was upregulated in the Si-LncMIAT group compared with the Si-NC and hypoxia groups (P < 0.01). Based on the aforementioned results, it was demonstrated that LncMIAT could regulate miR-708-5p in hypoxic cardiomyocytes.
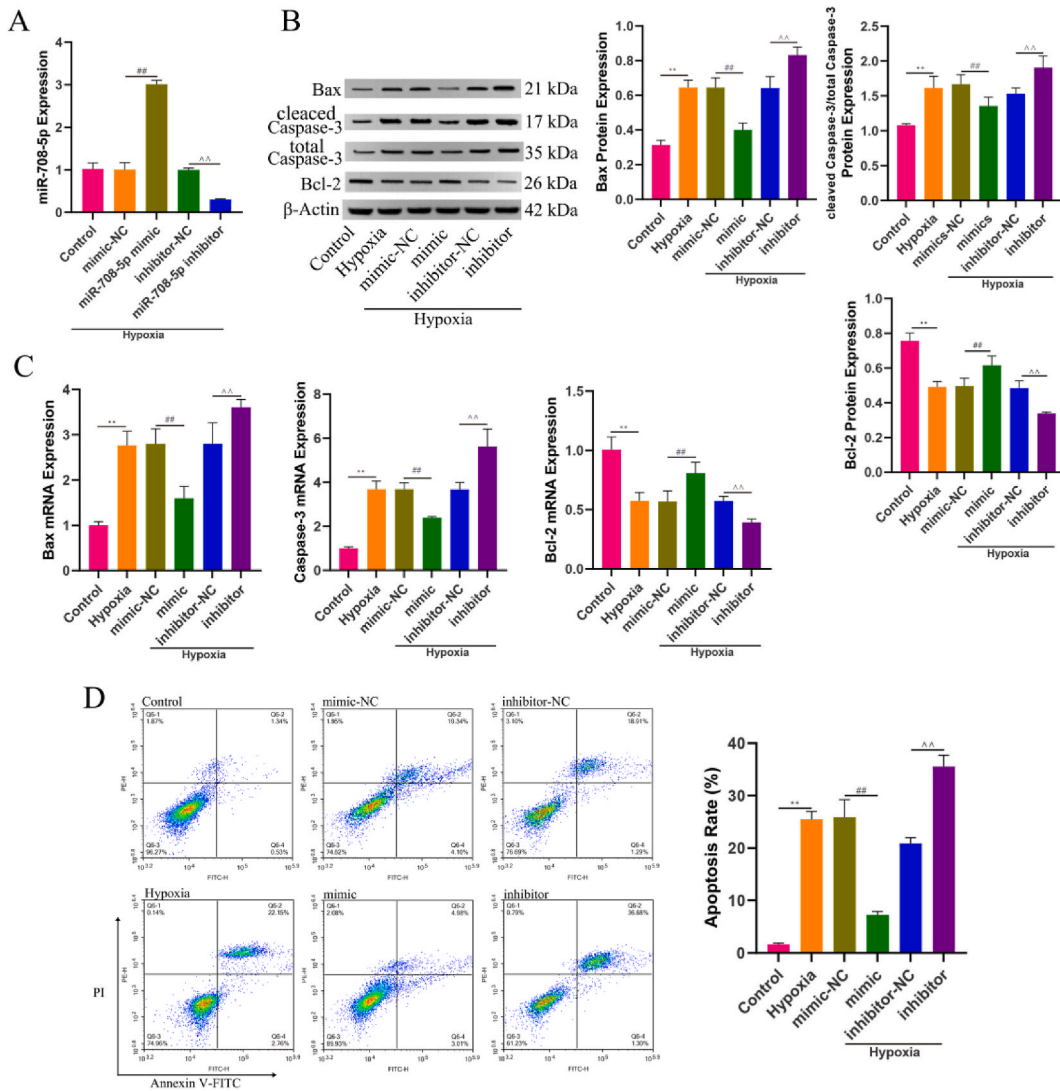

Fig. 5. MiR-708-5p affects the apoptosis of HL-1 cells under hypoxic conditions. Relative miR-708-5p expression in hypoxic HL-1 cells treated with (A) MiR-708-5p mimic and mimic-NC or MiR-708-5p inhibitor and inhibitor-NC. (B) Relative protein expression levels of Bax, cleaved Caspase-3 and Bcl-2. (C) Relative mRNA expression levels of Bax, Caspase-3 and Bcl-2. (D) Apoptotic rate of the HL-1 cells according to flow cytometric analysis. Data are shown as the mean ± standard deviation (n ≥ 3). **P < 0.01 vs. control group. ##P < 0.01 vs. mimic-NC group. ^^P < 0.01 vs. inhibitor-NC group.

3.5. miR-708-5p regulates cardiomyocyte apoptosis under hypoxic conditions

To elucidate whether miR-708-5p could influence the apoptotic rate of hypoxia-induced cardiomyocytes, HL-1 cells were transfected with a miR-708-5p mimic and a miR-708-5p inhibitor before inducing hypoxia. The expression of miR-708-5p was significantly increased in the miR-708-5p mimic group compared with that in the mimic-NC group (P < 0.01; Fig. 5A), and the expression of miR-708-5p was significantly decreased in miR-708-5p inhibitor group compared with that in the inhibitor-NC group (P < 0.01; Fig. 5A). The mRNA and protein expression levels of Bax (P < 0.01; Fig. 5B and C) were downregulated in the mimic group compared with the mimic-NC group. The protein expression level of cleaved Caspase-3 (P < 0.01; Fig. 5B) and mRNA expression level of Caspase-3 (P < 0.01; Fig. 5C) were decreased in the mimic group compared with the mimic-NC group. By contrast, the protein expression level of Bcl-2 (P < 0.01; Fig. 5B and C) were upregulated compared with the mimic-NC group. In addition, the mRNA and protein expression levels of Bax (P < 0.01; Fig. 5B and C) were increased in the inhibitor group compared with those in the inhibitor-NC group, whereas the protein expression level of Bcl-2 (P < 0.01; Fig. 5B and C) were decreased. The protein expression level of cleaved Caspase-3 (P < 0.01; Fig. 5B) and mRNA expression level of Caspase-3 (P < 0.01; Fig. 5C) were increased in the inhibitor group compared with those in the inhibitor-NC group. According to the flow cytometric analysis, the apoptotic rate in the mimic group was significantly decreased compared with that in the mimic-NC group, whereas the apoptotic ratio of the inhibitor group was significantly increased compared with the inhibitor-NC group (P < 0.01; Fig. 5D).

3.6. miR-708-5p endogenously binds with p53 mRNA in hypoxic cardiomyocytes

Subsequently, we sought to investigate whether miR-708-5p could regulate p53 in hypoxic cardiomyocytes. Fig. 6A depicts the predicted binding sites of miR-708-5p to the p53 mRNA sequence and the p53 mRNA mutation sequence. The luciferase activity was found to be significantly decreased in the p53-WT + miR-708-5p mimic group, but not in the p53-MUT + miR-708-5p mimic group (P < 0.01; Fig. 6B). The p53 mRNA and protein expression level was subsequently detected using RT-qPCR and Western blot analyses, respectively. The mRNA and protein expression levels of p53 were found to be decreased in the mimic group compared with those in
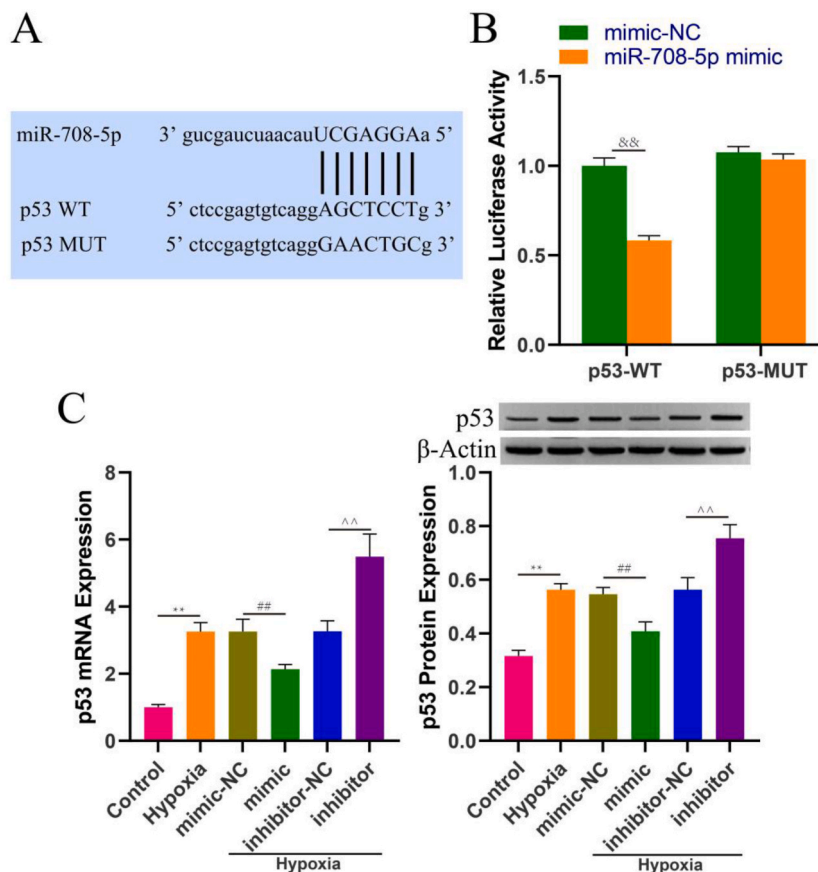

Fig. 6. MiR-708-5p endogenously binds with p53 mRNA to regulate p53 mRNA expression in hypoxic HL-1 cells. (A) Predicted binding site of miR-708-5p with p53 mRNA and mutant sequence of p53 mRNA. (B) Binding of miR-708-5p with p53 mRNA was detected using the dual luciferase reporter assay. (C) Relative mRNA and protein expression levels of p53. Data are shown as the mean ± standard deviation (n ≥ 3). &&P < 0.01 vs. mimic-NC group. **P < 0.01 vs. control group. ##P < 0.01 vs. mimic-NC group. ~P < 0.01 vs. inhibitor-NC group.
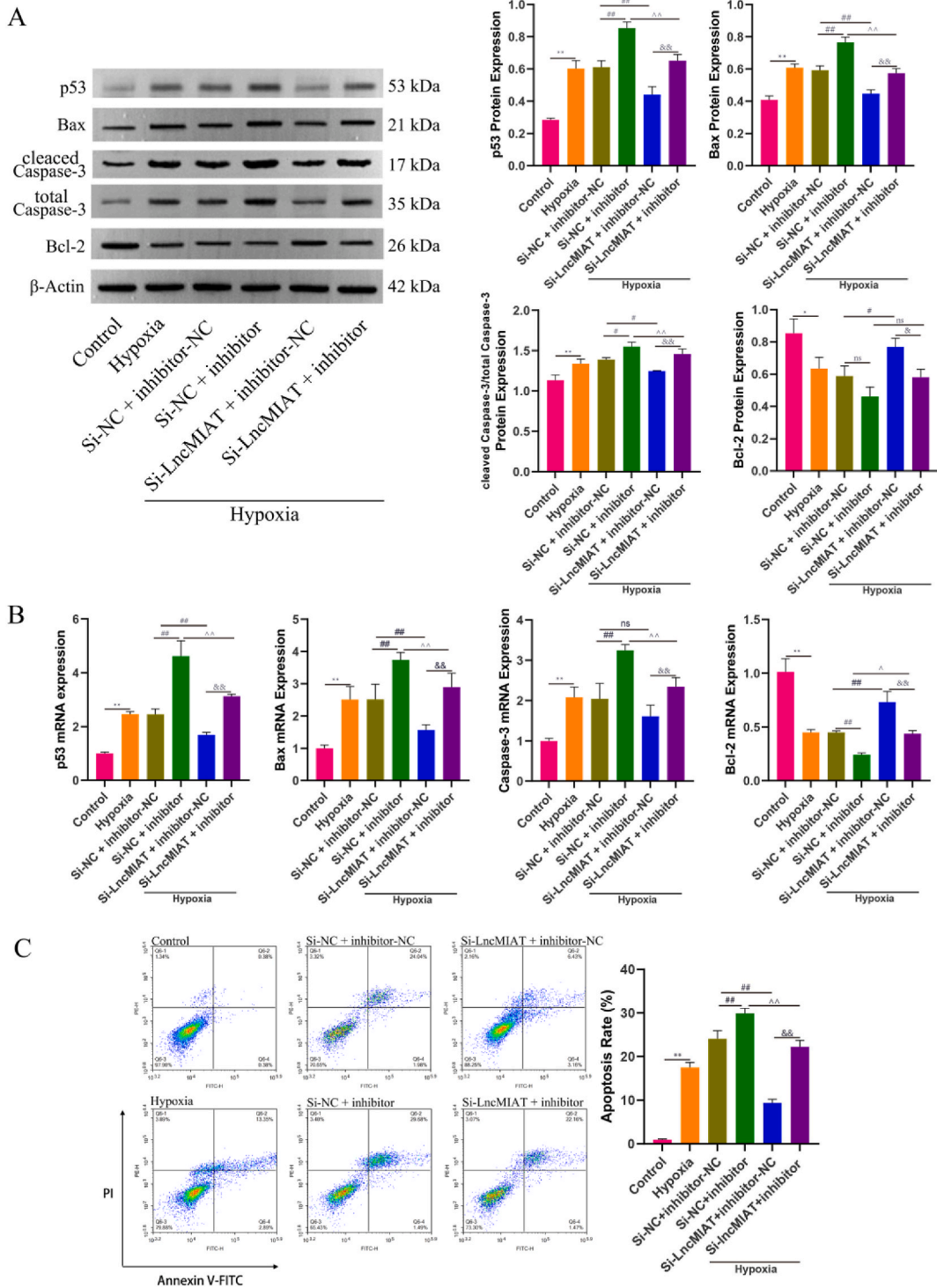
Fig. 7. LncMIAT binds to miR-708-5p and further regulates p53-induced cardiomyocyte apoptosis in hypoxic HL-1 cells. (A) Relative protein expression levels of P53, Bax, cleaved Caspase-3 and Bcl-2. (B) Relative mRNA expression levels of P53, Bax, Caspase-3 and Bcl-2. (C) Apoptotic rate of HL-1 cells according to flow cytometric analysis. Data are shown as the mean $\pm$ standard deviation (n $\geq$ 3). *P < 0.05 and **P < 0.01 vs. control group; #P < 0.05 and ##P < 0.01 vs. Si-NC + inhibitor-NC group; ^P < 0.05 and ^^P < 0.01 vs. Si-LncMIAT + inhibitor. &P < 0.05 and &&P < 0.01 vs. Si-LncMIAT + inhibitor-NC group.

the mimic-NC group (P < 0.01; Fig. 6C). By contrast, the mRNA and protein expression levels of p53 were increased in the inhibitor group compared with those in the inhibitor-NC group (P < 0.01; Fig. 6C). Collectively, these results suggested that miR-708-5p could regulate the expression of p53 mRNA in hypoxic cardiomyocytes.

3.7. Inhibition of LncMIAT suppresses p53 expression and apoptosis in cardiomyocytes by upregulating miR-708-5p in hypoxic HL-1 cells

Si-LncMIAT- and miR-708-5p inhibitor-transfected HL-1 cells were then generated to investigate the co-effects of LncMIAT and miR-708-5p in terms of cardiomyocyte apoptosis regulation. All silenced transfection groups were subjected to hypoxic conditions. The Si-LncMIAT + miR-708-5p inhibitor group exhibited significantly reduced mRNA and protein expression levels of p53 (P < 0.01; Fig. 7A and B) and Bax (P < 0.01; Fig. 7A and B) compared with the Si-NC + inhibitor group. The Si-LncMIAT + miR-708-5p inhibitor group exhibited significantly reduced protein expression level of cleaved Caspase-3 (P < 0.01; Fig. 7A) and mRNA expression level of Caspase-3 (P < 0.01; Fig. 7B) compared with the Si-NC + inhibitor group. By contrast, the Si-LncMIAT + miR-708-5p inhibitor group exhibited significantly increased Bcl-2 mRNA (P < 0.05) expression levels (Fig. 7B) compared with the Si-NC + inhibitor group. The Si-LncMIAT + miR-708-5p inhibitor group was found to exhibit significantly increased mRNA and protein expression levels of p53 (P < 0.01; Fig. 7A and B), Bax (P < 0.01; Fig. 7A and B), while decreasing Bcl-2 mRNA (P < 0.01) and Bcl-2 protein (P < 0.05) expression levels (Fig. 7A and B) compared with the Si-LncMIAT + inhibitor-NC group. The Si-LncMIAT + miR-708-5p inhibitor group exhibited significantly increased protein expression level of cleaved Caspase-3 (P < 0.01; Fig. 7A) and mRNA expression level of Caspase-3 (P < 0.01; Fig. 7B) compared with the Si-LncMIAT + inhibitor-NC group. According to the flow cytometry experiments, the Si-LncMIAT + miR-708-5p inhibitor group showed a significantly decreased apoptotic ratio compared with the Si-NC + inhibitor group (P < 0.01), whereas the Si-LncMIAT + miR-708-5p inhibitor group showed a significant increase in the apoptotic ratio compared with the Si-LncMIAT + inhibitor-NC group (P < 0.01; Fig. 7C). Taken together, the aforementioned results demonstrated the interplay that occurred between LncMIAT and miR-708-5p in terms of their influencing p53-induced cardiomyocyte apoptosis under hypoxic conditions.
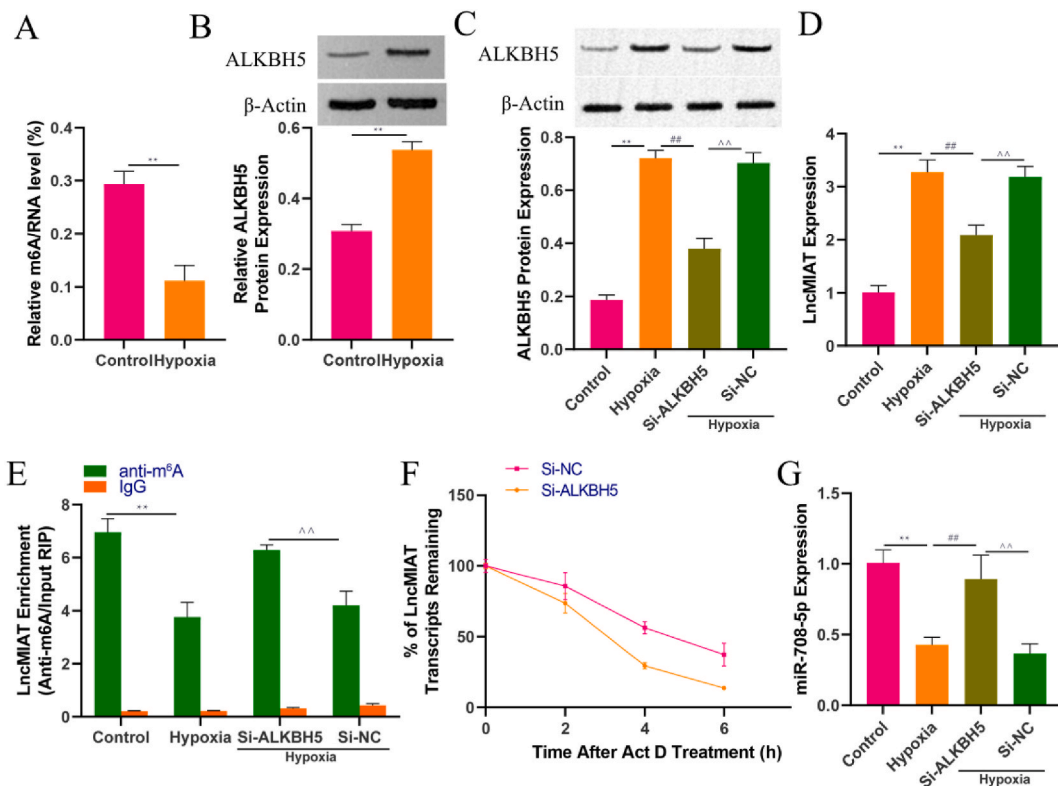

Fig. 8. Inhibition of ALKBH5 increases the m⁶A methylation level of LncMIAT and further reduces LncMIAT expression in hypoxic HL-1 cells. (A) Percentage of total m⁶A in the total RNA according to the m⁶A RNA methylation quantification assay. (B) Enhancement of the AKLBH5 relative protein expression level following the hypoxia stimulus. (C) ALKBH5 protein expression level following ALKBH5 silencing. (D) LncMIAT expression following ALKBH5 silencing. (E) M⁶A methylation level of LncMIAT was determined using MeRIP-qPCR analysis. (F) The remaining LncMIAT transcripts following silence of ALKBH5. (G) MiR-708-5p expression following ALKBH5 silencing. Data are shown as the mean ± standard deviation (n ≥ 3). **P < 0.01 vs. control group. ##P < 0.01 vs. hypoxia group. ˜P < 0.01 vs. Si-ALKBH5 group.

3.8. The m⁶A modification is associated with hypoxia-mediated LncMIAT variations regulated by ALKBH5 in vitro

The results of the m^{6}A colorimetric quantification assay showed that hypoxia-treated HL-1 cells exhibited a significantly decreased m^{6}A methylation level in total RNA compared with the control group (P < 0.01; Fig. 8A). The ALKBH5 protein expression level was significantly increased under hypoxia condition (P < 0.01; Fig. 8B), indicating that ALKBH5 could negatively regulate the m^{6}A methylation level. Subsequently, ALKBH5 silencing was effectively established (P < 0.01; Fig. 8C) and the LncMIAT expression level was significantly lowered (P < 0.01; Fig. 8D) under hypoxic conditions. The MeRIP-qPCR test under hypoxic conditions was then performed on Si-ALKBH5-transfected HL-1 cells to understand the association between ALKBH5, m^{6}A methylation and LncMIAT. The results obtained showed that inhibiting ALKBH5 decreased the expression of LncMIAT by regulating LncMIAT m^{6}A methylation (P < 0.01; Fig. 8E). Actinomycin D (ActD) results were subsequently showed that transfection with Si-ALKBH5 reduced the remaining stability of LncMIAT compared with that in the Si-NC group (Fig. 8F). Moreover, Si-ALKBH5 significantly increased miR-708-5p (P < 0.01; Fig. 8G) levels under hypoxia. Collectively, these experiments indicated that ALKBH5 inhibits the degradation process of LncMIAT by downregulating the m^{6}A methylation of LncMIAT in cardiomyocytes under hypoxic conditions.
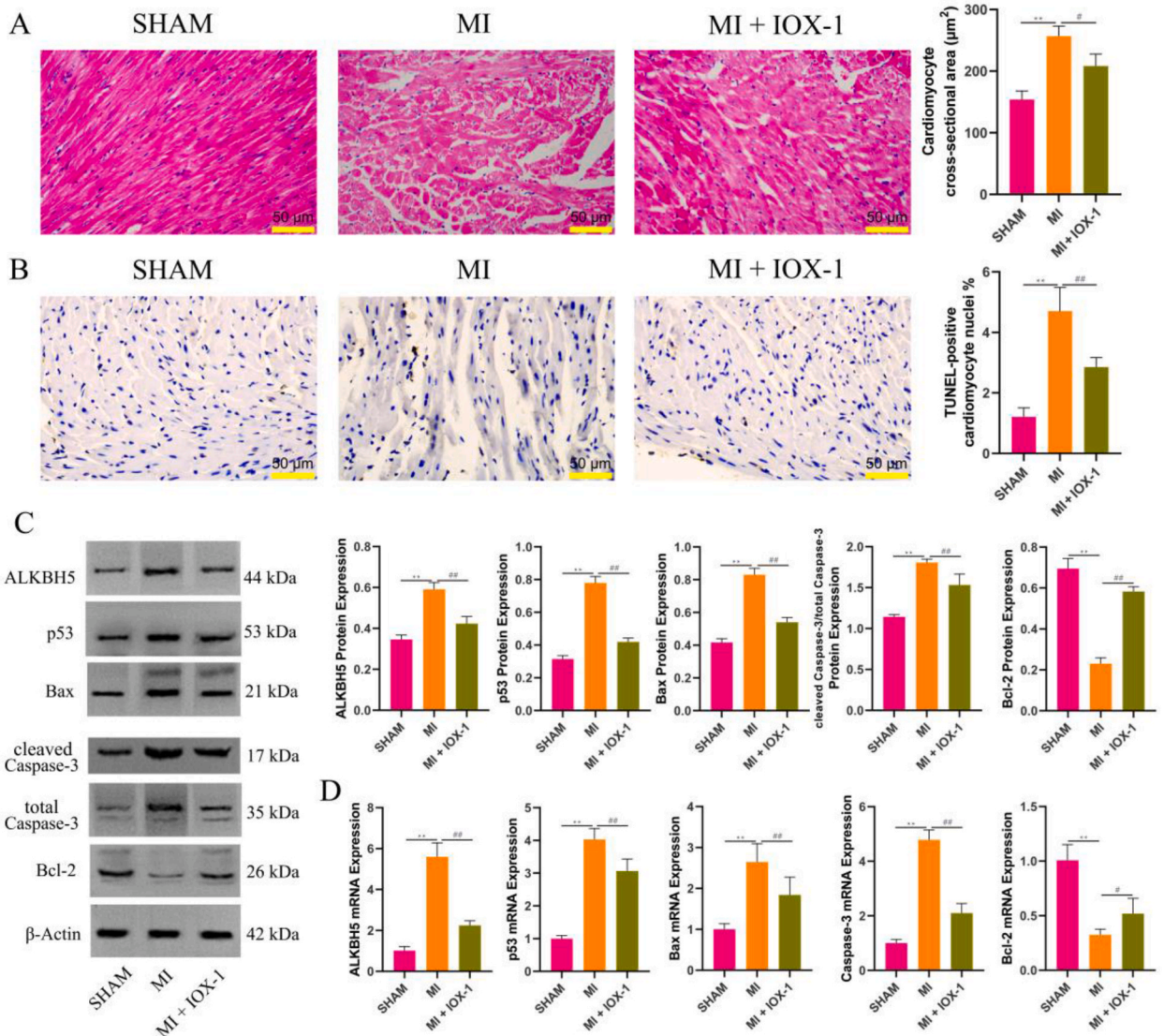

Fig. 9. ALKBH5 inhibitor IOX-1 regulates the p53 expression and myocardial apoptosis in an MI mice model. (A) Histological changes were measured using H&E staining (scale bar, 50 μm). (B) Changes in the apoptotic rate were measured using TUNEL assay (scale bar, 50 μm). (C) Relative protein expression levels of ALKBH5, P53, Bax, cleaved Caspase-3 and Bcl-2. (D) Relative mRNA expression levels of ALKBH5, P53, Bax, Caspase-3 and Bcl-2. Data are shown as the mean ± standard deviation (n ≥ 3). **P < 0.01 vs. SHAM group. #P < 0.05 and ##P < 0.01 vs. MI group.

3.9. Hypoxia-mediated myocardial apoptosis is regulated by the ALKBH5 inhibitor IOX-1 via p53 in an MI mice model

IOX-1 was intragastrically administered to MI model mice to confirm whether the changes in m^6A methylation-mediated LncMIAT and the LncMIAT/miR-708-5p/p53 axis that mediates cardiomyocyte apoptosis were regulated by ALKBH5 *in vivo*. As expected and shown through H&E and TUNEL staining assays, treatment with the ALKBH5 inhibitor IOX-1 significantly reduced the cardiomyocyte cross-sectional area ($P < 0.05$; Fig. 9A) and apoptosis ratio ($P < 0.01$; Fig. 9B). Subsequently, the administration of IOX-1 significantly reduced ALKBH5 mRNA and protein expression levels ($P < 0.01$; Fig. 9C and D). Further results showed that the IOX-1 significantly reduced mRNA and protein expression levels of p53 ($P < 0.01$; Fig. 9C and D) and Bax ($P < 0.01$; Fig. 9C and D) level. In addition, the IOX-1 significantly reduced protein expression level of cleaved Caspase-3 ($P < 0.01$; Fig. 9C) and mRNA expression level of Caspase-3 ($P < 0.01$; Fig. 9D) compared with the MI group. By contrast, the Bcl-2 mRNA ($P < 0.05$) and Bcl-2 protein ($P < 0.01$) expression levels (Fig. 9C and D) were significantly increased compared with the MI group. Taken together, these experiments demonstrated that the ALKBH5 inhibitor IOX-1 could regulate the m^6A methylation of LncMIAT, which mediated alterations in the p53 expression level and further affected cardiomyocyte apoptosis in an MI model under hypoxia conditions *in vivo*.

4. Discussion

The present study firstly explored the hypoxia-mediated cardiomyocyte apoptosis via p53 *in vitro* and *in vivo*. Then, through bioinformatics analysis, dual luciferase gene report assay and RNA silencing and overexpression, the LncMIAT/miR-708-5p/p53 axis has been shown to regulate hypoxia-mediated cardiomyocyte apoptosis. Finally, we found that the alterations in the m6A methylation-mediated LncMIAT/miR-708-5p/p53 axis and myocardial apoptosis were regulated by ALKBH5 under hypoxic conditions.

MI is the major cause of myocardial cell injury and death [34,35]. To mimic the MI model *in vitro*, in the present study, HL-1 cardiomyocytes were subjected to a hypoxic environment for 24 h. HIF-1α upregulation was investigated to confirm that the hypoxic cardiomyocyte model had been successfully established. Generally, cardiomyocyte apoptosis exerts an important role in the exacerbation of MI [36]. The basic mechanism associated with cardiomyocyte apoptosis features crucial changes to the mediator protein Bax and activation of caspase-3, whereas the level of Bcl-2 is inhibited [24,37,38]. In the present study, the apoptotic rate was significantly increased following the hypoxia stimulus, as observed through flow cytometric analysis. Moreover, significant increases in Bax and caspase-3 expression were observed, whereas Bcl-2 expression was decreased in the hypoxic HL-1 cells. These results demonstrated that the hypoxia stimulus could promote cardiomyocyte apoptosis compared with normoxic conditions. Generally, p53 serves to activate the tumor suppressor, mouse double minute 2 and PTEN expression-induced apoptosis [39]. In the myocardium, the activation of p53 was shown to aggravate MI injury and to increase the level of apoptosis, as determined by changes to the Bax/Bcl-2 ratio and caspase-3 activation [11,40]. In the present study, the level of p53 was measured to determine how the hypoxia stimulus could regulate p53-induced apoptosis in cardiomyocytes. The results obtained showed that the hypoxia stimulus promoted p53 expression in the cardiomyocytes. Collectively, the aforementioned results demonstrated that the hypoxia stimulus could exacerbate cardiomyocyte apoptosis by regulating p53 expression.

LncMIAT, a high-sensitivity biomarker for myocardial disease in the plasma and tissues of both patients and animals, is particularly associated with MI [18,41]. In this study, we confirmed the upregulation of LncMIAT through bioinformatics analysis of blood samples from MI patients. The level of LncMIAT was also found to be increased in hypoxic HL-1 cardiomyocytes. Generally, cardiomyocyte apoptosis exerts an important role in the exacerbation of MI [36]. Although we and others have identified the upregulation of LncMIAT in MI diseases, the impact of LncMIAT expression on cardiomyocyte apoptosis remains unclear. In this study, LncMIAT inhibition was shown to protect hypoxic cardiomyocytes from apoptosis, as determined by alterations in the levels of the apoptotic mediators Bax, Bcl-2 and caspase-3 via p53 protein. MiR-708-5p is a biomarker in myocardial infarction that promoted cardiomyocyte proliferation in a neonatal mouse model [26]. The present study demonstrated that the induced hypoxia led to a significant decrease in miR-708-5p expression in HL-1 cardiomyocytes. Furthermore, overexpressing miR-708-5p ameliorated the apoptotic changes in hypoxia-treated cardiomyocytes, whereas the inhibition of miR-708-5p increased cell apoptosis via p53 protein. These findings added further evidence to support that miR-708-5p inhibits apoptosis in cardiomyocytes via p53. Subsequently, to confirm whether any interaction occurred between miR-708-5p with LncMIAT and p53 mRNA, the existence of high-degree endogenous RNA-binding sites between LncMIAT, miR-708-5p and p53 mRNA was investigated after using a prediction tool. The luciferase gene report assay showed that miR-708-5p did bind with LncMIAT and p53 mRNA, indicating that LncMIAT may negatively regulate miR-708-5p, which consequently inhibits p53 mRNA expression. Therefore, the possibility arose that LncMIAT could regulate myocardial apoptosis via the LncMIAT/miR-708-5p/p53 axis. To further elucidate the co-operative effects of LncMIAT and miR-708-5p in terms of regulating p53-induced myocardial apoptosis, a rescue experiment employing silencing of LncMIAT and miR-708-5p inhibitor was performed. The inhibition of miR-708-5p with Si-LncMIAT led to an alteration in the protein and mRNA expression of p53, and in the level of apoptotic rate and proteins. Therefore, these findings added further supported that LncMIAT increased p53 expression-mediated apoptosis in hypoxic cardiomyocytes by decreasing the level of miR-708-5p.

In myocardial research, m^6A methylation is a highly adaptable type of modification that is regulated by either N^6-adenosine methyltransferase or demethylase. Previous studies have shown that m^6A RNA methylation was significantly reduced in MI [42,43]. The current m^6A quantification assay results confirmed that the level of myocardial m^6A methylation was significantly reduced by the hypoxia stimulus. Several studies showed that the m^6A methylation of adenosines level was regulated by METTL3 and METTL14 in ischemic heart disease [43,44]. A recent study also showed that ALKBH5 reduced m^6A methylation in ischemic endothelial cells [45]. However, the function and the underlying mechanism of the ALKBH5 in hypoxic cardiomyocytes have not been elucidated. To investigate the effect of ALKBH5 on m^6A methylation in hypoxic cardiomyocytes, the ALKBH5 level was subsequently measured,

which exhibited a significant increase compared with the normoxic control. A recent study suggested that m[6]A methylation could influence the expression of LncMIAT [46]. Notably, intensive studies showed that ALKBH5 can regulate the m[6]A methylation of lncRNAs, further affecting their expression and function [47–49]. However, the role of m[6]A demethylation of LncMIAT regulated by ALKBH5 in hypoxic myocardium disease is largely unknown. Thus, the present study measured the LncMIAT level following ALKBH5 inhibition under hypoxic conditions and the results obtained showed a significantly decreased level of LncMIAT following silencing of ALKBH5. Thus, the present study found that the inhibition of ALKBH5 significantly decreased level of LncMIAT under hypoxic conditions *in vitro*. MeRIP-qPCR analysis confirmed that the ALKBH5 could facilitate LncMIAT expression by reducing m[6]A methylation, both *in vitro* and *in vivo*. These findings, therefore, suggested that ALKBH5 inhibits m[6]A methylation while promoting LncMIAT expression in hypoxic cardiomyocytes. Finally, the effects of the ALKBH5 inhibitor, IOX-1, on changes in the LncMIAT/miR-708-5p/p53 axis and myocardial apoptosis were investigated *in vivo*. The results showed that the alterations in the m[6]A methylation-mediated LncMIAT/miR-708-5p/p53 axis and the further enhanced myocardial apoptosis were regulated by ALKBH5 under hypoxic conditions. However, additional research to fully delineate the underlying mechanism of m[6]A methylation modification in regulating LncMIAT expression is required.

5. Conclusions

In summary, the present study showed that hypoxia stimulus could promote cardiomyocyte apoptosis via the LncMIAT/miR-708-5p/p53 signaling axis. Moreover, an increase in the level of LncMIAT was associated with a decrease in ALKBH5-mediated m[6]A methylation (Fig. 10). The present study highlighted LncMIAT as a potential target for detecting myocardial apoptosis; however, further studies are required to elucidate the precise mechanism underlying the hypoxia regulation of ALKBH5 and LncMIAT m[6]A methylation.

Ethical statement

All experimental protocols were approved by the Animal Experimentation Ethics Committee of the Anhui University of Chinese Medicine (approval no. AHUCM-mouse-2022009) and conducted following the EU Directive 2010/63/EU guideline.

Data availability statement

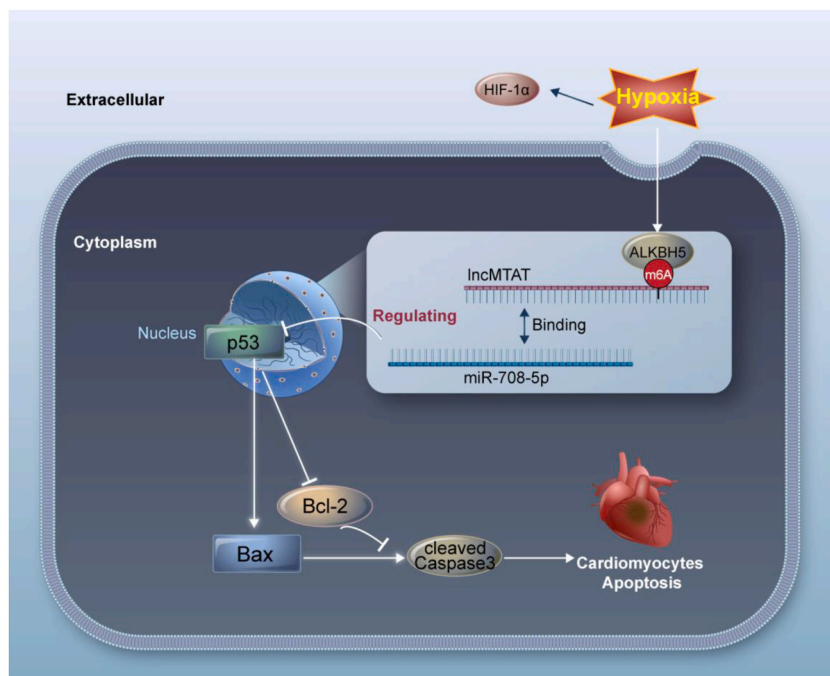Data included in article/supp. material/referenced in article.

Fig. 10. Schematic diagram of hypoxia triggers the N[6]-methyladenosine methylation-mediated LncMIAT/miR-708-5p/p53 axis before cardiomyocyte apoptosis.

Disclosure statement

The authors declare that the research was conducted in the absence of any commercial or financial relationships that could be construed as a potential conflict of interest.

Funding

CRediT authorship contribution statement

Chuqiao Shen: Writing – review & editing, Writing – original draft, Methodology, Investigation, Funding acquisition, Formal analysis, Data curation. **Xiaoqi Chen:** Writing – original draft, Investigation, Data curation. **Yixuan Lin:** Visualization, Formal analysis, Data curation. **Yan Yang:** Writing – review & editing, Supervision, Project administration, Conceptualization.

Declaration of competing interest

The authors declare that they have no known competing financial interests or personal relationships that could have appeared to influence the work reported in this paper.

Acknowledgements

Appendix A. Supplementary data

Supplementary data to this article can be found online at https://doi.org/10.1016/j.heliyon.2024.e32455.

References

[1] G.A. Roth, G.A. Mensah, C.O. Johnson, et al., Global burden of cardiovascular diseases and risk factors, 1990-2019: update from the GBD 2019 study, J. Am. Coll. Cardiol. 76 (2020) 2982–3021, https://doi.org/10.1016/j.jacc.2020.11.010.

[2] A.L. Bui, T.B. Horwich, G.C. Fonarow, Epidemiology and risk profile of heart failure, Nat. Rev. Cardiol. 8 (2011) 30–41, https://doi.org/10.1038/nrcardio.2010.165.

[3] H. Yu, B. Chen, Q. Ren, Baicalin relieves hypoxia-aroused H9c2 cell apoptosis by activating Nrf2/HO-1-mediated HIF1alpha/BNIP3 pathway, Artif. Cells, Nanomed. Biotechnol. 47 (2019) 3657–3663, https://doi.org/10.1080/21691401.2019.1657879.

[4] A. Shekhar, P. Heeger, C. Reutelingsperger, et al., Targeted imaging for cell death in cardiovascular disorders, JACC Cardiovasc Imaging 11 (2018) 476–493, https://doi.org/10.1016/j.jcmg.2017.11.018.

[5] D. Zhang, C. Jiang, Y. Feng, et al., Molecular imaging of myocardial necrosis: an updated mini-review, J. Drug Target. 28 (2020) 565–573, https://doi.org/10.1080/1061186X.2020.1725769.

[6] L. Hofstra, I.H. Liem, E.A. Dumont, et al., Visualisation of cell death in vivo in patients with acute myocardial infarction, Lancet 356 (2000) 209–212, https://doi.org/10.1016/s0140-6736(00)02482-x.

[7] D.E. Sosnovik, E.A. Schellenberger, M. Nahrendorf, et al., Magnetic resonance imaging of cardiomyocyte apoptosis with a novel magneto-optical nanoparticle, Magn. Reson. Med. 54 (2005) 718–724, https://doi.org/10.1002/mrm.20617.

[8] D.P. Del Re, D. Amgalan, A. Linkermann, et al., Fundamental mechanisms of regulated cell death and implications for heart disease, Physiol. Rev. 99 (2019) 1765–1817, https://doi.org/10.1152/physrev.00022.2018.

[9] F. Sun, J. Du, H. Li, et al., FABP4 inhibitor BMS309403 protects against hypoxia-induced H9c2 cardiomyocyte apoptosis through attenuating endoplasmic reticulum stress, J. Cell Mol. Med. 24 (2020) 11188–11197, https://doi.org/10.1111/jcmm.15666.

[10] L. Zhang, Y.N. Wang, J.M. Ju, et al., Mzb1 protects against myocardial infarction injury in mice via modulating mitochondrial function and alleviating inflammation, Acta Pharmacol. Sin. 42 (2021) 691–700, https://doi.org/10.1038/s41401-020-0489-0.

[11] M. Ikeda, T. Ide, T. Tadokoro, et al., Excessive hypoxia-inducible factor-1alpha expression induces cardiac rupture via p53-dependent apoptosis after myocardial infarction, J. Am. Heart Assoc. 10 (2021) e020895, https://doi.org/10.1161/JAHA.121.020895.

[12] X. Zhang, Z. Qi, H. Yin, et al., Interaction between p53 and Ras signaling controls cisplatin resistance via HDAC4- and HIF-1alpha-mediated regulation of apoptosis and autophagy, Theranostics 9 (2019) 1096–1114, https://doi.org/10.7150/thno.29673.

[13] K.B. Leszczynska, I.P. Foskolou, A.G. Abraham, et al., Hypoxia-induced p53 modulates both apoptosis and radiosensitivity via AKT, J. Clin. Invest. 125 (2015) 2385–2398, https://doi.org/10.1172/JCI80402.

[14] Y. Ge, S. Wu, Z. Zhang, et al., Inhibition of p53 and/or AKT as a new therapeutic approach specifically targeting ALT cancers, Protein Cell 10 (2019) 808–824, https://doi.org/10.1007/s13238-019-0634-z.

[15] H.J. Shi, M.W. Wang, J.T. Sun, et al., A novel long noncoding RNA FAF inhibits apoptosis via upregulating FGF9 through PI3K/AKT signaling pathway in ischemia-hypoxia cardiomyocytes, J. Cell. Physiol. 234 (2019) 21973–21987, https://doi.org/10.1002/jcp.28760.

[16] M. Vausort, D.R. Wagner, Y. Devaux, Long noncoding RNAs in patients with acute myocardial infarction, Circ. Res. 115 (2014) 668–677, https://doi.org/10.1161/CIRCRESAHA.115.303836.

[17] M.Y. Elwazir, M.H. Hussein, E.A. Toraih, et al., Association of angio-LncRNAs MIAT rs1061540/MALAT1 rs3200401 molecular variants with gensini score in coronary artery disease patients undergoing angiography, Biomolecules 12 (2022), https://doi.org/10.3390/biom12010137.

[18] M. Azat, X. Huojiahemaiti, R. Gao, et al., Long noncoding RNA MIAT: a potential role in the diagnosis and mediation of acute myocardial infarction, Mol. Med. Rep. 20 (2019) 5216–5222, https://doi.org/10.3892/mmr.2019.10768.

[19] X. Bai, C. Yang, L. Jiao, et al., LncRNA MIAT impairs cardiac contractile function by acting on mitochondrial translocator protein TSPO in a mouse model of myocardial infarction, Signal Transduct. Targeted Ther. 6 (2021) 172, https://doi.org/10.1038/s41392-021-00538-y.

[20] L. Yang, J. Deng, W. Ma, et al., Ablation of lncRNA Miat attenuates pathological hypertrophy and heart failure, Theranostics 11 (2021) 7995–8007, https://doi.org/10.7150/thno.50990.

[21] L. Cong, Y. Su, D. Wei, et al., Catechin relieves hypoxia/reoxygenation-induced myocardial cell apoptosis via down-regulating lncRNA MIAT, J. Cell Mol. Med. 24 (2020) 2356–2368, https://doi.org/10.1111/jcmm.14919.

[22] L. Chen, D. Zhang, L. Yu, et al., Targeting MIAT reduces apoptosis of cardiomyocytes after ischemia/reperfusion injury, Bioengineered 10 (2019) 121–132, https://doi.org/10.1080/21655979.2019.1605812.

[23] X. Cao, Q. Ma, B. Wang, et al., Silencing long non-coding RNA MIAT ameliorates myocardial dysfunction induced by myocardial infarction via MIAT/miR-10a-5p/EGR2 axis, Aging 13 (2021) 11188–11206, https://doi.org/10.18632/aging.202785.

[24] F. Cheng, W. Yuan, M. Cao, et al., Cyclophilin A protects cardiomyocytes against hypoxia/reoxygenation-induced apoptosis via the AKT/nox 2 pathway, Oxid. Med. Cell. Longev. 2019 (2019) 2717986, https://doi.org/10.1155/2019/2717986.

[25] S. Zhang, Y. Wang, P. Wang, et al., miR-708 affords protective efficacy in anoxia/reoxygenation-stimulated cardiomyocytes by blocking the TLR4 signaling via targeting HMGB1, Mol. Cell. Probes 54 (2020) 101653, https://doi.org/10.1016/j.mcp.2020.101653.

[26] S. Deng, Q. Zhao, L. Zhen, et al., Neonatal heart-enriched miR-708 promotes proliferation and stress resistance of cardiomyocytes in rodents, Theranostics 7 (2017) 1953–1965, https://doi.org/10.7150/thno.16478.

[27] Y. Wang, M. Xu, P. Yue, et al., Novel insights into the potential mechanisms of N6-methyladenosine RNA modification on sepsis-induced cardiovascular dysfunction: an update summary on direct and indirect evidences, Front. Cell Dev. Biol. 9 (2021) 772921, https://doi.org/10.3389/fcell.2021.772921.

[28] S. Wu, S. Zhang, X. Wu, et al., m(6)A RNA methylation in cardiovascular diseases, Mol. Ther. 28 (2020) 2111–2119, https://doi.org/10.1016/j.ymthe.2020.08.010.

[29] Y. Zhao, J. Hu, X. Sun, et al., Loss of m6A demethylase ALKBH5 promotes post-ischemic angiogenesis via post-transcriptional stabilization of WNT5A, Clin. Transl. Med. 11 (2021) e402, https://doi.org/10.1002/ctm2.402.

[30] E. Parliament, E. Council, DIRECTIVE 2010/63/EU on the Protection of Animals Used for Scientific Purposes, 2010.

[31] Z. Shen, A. Shen, X. Chen, et al., Huoxin pill attenuates myocardial infarction-induced apoptosis and fibrosis via suppression of p53 and TGF-beta 1/Smad 2/3 pathways, Biomed. Pharmacother. 130 (2020) 110618, https://doi.org/10.1016/j.biopha.2020.110618.

[32] Y. Deng, M. Li, M. Zhuo, et al., Histone demethylase JMJD2D promotes the self-renewal of liver cancer stem-like cells by enhancing EpCAM and Sox 9 expression, J. Biol. Chem. 296 (2021) 100121, https://doi.org/10.1074/jbc.RA120.015335.

[33] F. Li, S. Kennedy, T. Hajian, et al., A radioactivity-based assay for screening human m6A-RNA methyltransferase, METTL3-METTL14 complex, and demethylase ALKBH5, J. Biomol. Screen 21 (2016) 290–297, https://doi.org/10.1177/1087057115623264.

[34] D.O. Okonko, A.M. Shah, Heart failure: mitochondrial dysfunction and oxidative stress in CHF, Nat. Rev. Cardiol. 12 (2015) 6–8, https://doi.org/10.1038/nrcardio.2014.189.

[35] J.L. Anderson, D.A. Morrow, Acute myocardial infarction, N. Engl. J. Med. 376 (2017) 2053–2064, https://doi.org/10.1056/NEJMra1606915.

[36] Q. Zhang, L. Wang, S. Wang, et al., Signaling pathways and targeted therapy for myocardial infarction, Signal Transduct. Targeted Ther. 7 (2022) 78, https://doi.org/10.1038/s41392-022-00925-z.

[37] H. Cheng, S. Chang, R. Xu, et al., Hypoxia-challenged MSC-derived exosomes deliver miR-210 to attenuate post-infarction cardiac apoptosis, Stem Cell Res. Ther. 11 (2020) 224, https://doi.org/10.1186/s13287-020-01737-0.

[38] X. Wang, Z. Guo, Z. Ding, et al., Inflammation, autophagy, and apoptosis after myocardial infarction, J. Am. Heart Assoc. 7 (2018), https://doi.org/10.1161/JAHA.117.008024.

[39] H. Men, H. Cai, Q. Cheng, et al., The regulatory roles of p53 in cardiovascular health and disease, Cell. Mol. Life Sci. 78 (2021) 2001–2018, https://doi.org/10.1007/s00018-020-03694-6.

[40] T. Yagudin, Y. Zhao, H. Gao, et al., iASPP protects the heart from ischemia injury by inhibiting p53 expression and cardiomyocyte apoptosis, Acta Biochim. Biophys. Sin. 53 (2021) 102–111, https://doi.org/10.1093/abbs/gmaa104.

[41] F. Fasolo, H. Jin, G. Winski, et al., Long noncoding RNA MIAT controls advanced atherosclerotic lesion formation and plaque destabilization, Circulation 144 (2021) 1567–1583, https://doi.org/10.1161/CIRCULATIONAHA.120.052023.

[42] X. Su, Y. Shen, Y. Jin, et al., Aging-associated differences in epitranscriptomic m6A regulation in response to acute cardiac ischemia/reperfusion injury in female mice, Front. Pharmacol. 12 (2021) 654316, https://doi.org/10.3389/fphar.2021.654316.

[43] Y. Su, R. Xu, R. Zhang, et al., N6-methyladenosine methyltransferase plays a role in hypoxic preconditioning partially through the interaction with lncRNA H19, Acta Biochim. Biophys. Sin. 52 (2020) 1306–1315, https://doi.org/10.1093/abbs/gmaa130.

[44] P. Pang, Z. Qu, S. Yu, et al., Mettl14 attenuates cardiac ischemia/reperfusion injury by regulating wnt 1/beta-catenin signaling pathway, Front. Cell Dev. Biol. 9 (2021) 762853, https://doi.org/10.3389/fcell.2021.762853.

[45] R. Kumari, R. Dutta, P. Ranjan, et al., ALKBH5 regulates SPHK1-dependent endothelial cell angiogenesis following ischemic stress, Front Cardiovasc Med 8 (2021) 817304, https://doi.org/10.3389/fcvm.2021.817304.

[46] G. Steponaitis, R. Stakaitis, I. Valiulyte, et al., Transcriptome-wide analysis of glioma stem cell specific m6A modifications in long-non-coding RNAs, Sci. Rep. 12 (2022) 5431, https://doi.org/10.1038/s41598-022-08616-z.

[47] S. Zhang, B.S. Zhao, A. Zhou, et al., m(6)A demethylase ALKBH5 maintains tumorigenicity of glioblastoma stem-like cells by sustaining FOXM1 expression and cell proliferation program, Cancer Cell 31 (2017) 591–606 e596, https://doi.org/10.1016/j.ccell.2017.02.013.

[48] F. Dong, X. Qin, B. Wang, et al., ALKBH5 facilitates hypoxia-induced paraspeckle assembly and IL8 secretion to generate an immunosuppressive tumor microenvironment, Cancer Res. 81 (2021) 5876–5888, https://doi.org/10.1158/0008-5472.CAN-21-1456.

[49] Q. Wu, H. Zhang, D. Yang, et al., The m6A-induced lncRNA CASC8 promotes proliferation and chemoresistance via upregulation of hnRNPL in esophageal squamous cell carcinoma, Int. J. Biol. Sci. 18 (2022) 4824–4836, https://doi.org/10.7150/ijbs.71234.